Development of a Dynamic Model of the Egyptian Power Grid for AGC Studies Using Real Data

Radwa I. Soliman
National Energy Control Center
Egyptian Electricity
Transmission Company
Cairo, Egypt
roody_rfr2020@yahoo.com

Omar H. Abdalla
Dept. of Electrical Power and
Machines Enginneering
Helwan University
Cairo, Egypt
ohabdalla@ieee.org

Adel A. Emary
National Energy Control Center
Egyptian Electricity
Transmission Company
Cairo, Egypt
adelaly188@yahoo.com

Laila A. Talat
Dept. of Electrical Power and
Machines Enginneering
Helwan University
Cairo, Egypt
laila.talat@yahoo.com

***Abstract*—The paper presents the development of a dynamic model of the Egyptian power system for Automatic Generation Control (AGC) studies. Each category of turbine and its speed-governor system is lumped in an equivalent model. Parameters of each equivalent model are derived based on weighted-average real data. The Egyptian power grid is briefly described and the MATLAB/Simulink software is used to perform AGC studies. Governor dead-band and ramp rate are considered. Two operating conditions are studied: peak summer demand and minimum winter demand. An integral controller is designed and applied to the generating units under AGC control through a secondary loop. The primary loop is the conventional speed droop proportional control. Various scenarios of the frequency control are considered including AGC on different generating units. The simulation results have shown that the parameters of the proposed model are insensitive to variations in the system operating point, thus implying the validity of the model over a wide range of operating conditions.**

Keywords—Automatic Generation Control (AGC), Primary Frequency Control, Load Frequency Control (LFC), Egyptian Grid, Dead Band, Ramp Rate.

I. Introduction

Automatic Generation Control (AGC) [1] have been an active research topic over decades and will continue to be developed to precisely control the frequency in modern large power systems [2], [3]. In general, frequency control can be divided into three levels, namely primary frequency control, secondary frequency control and tertiary frequency control. Following a large disturbance, such as a generating unit trip or sudden connection of a large load, the imbalance of active power will be compensated from the kinetic energy of the rotating generating units leading to frequency decline. If the deviation in the frequency exceeds the governor dead-band, the primary frequency control starts through the speed governor systems of generators to increase their power outputs to compensate the power mismatch. With the conventional speed droop, the frequency will stabiles at a quasi-steady state value. If this quasi-steady frequency is outside the allowable normal operation frequency limit, the secondary frequency control will act to bring the frequency back to its normal operating limits. This secondary frequency control is known as AGC or Load Frequency Control (LFC) [4]. It is implemented centrally and applied only to generating units under this type of frequency control. The purpose of the tertiary control is to ensure economic operation of the power system. In most of AGC studies, simple models of power systems available in textbooks [5], [6] are used, but studies based on models of real power systems are rare.

The objective of this paper is to present a dynamic model of the Egyptian power system for AGC studies using real data. Each type of generating units is represented as a lumped equivalent model with weighted-average parameter values. Two operating scenarios are considered, namely peak load and minimum load conditions. Aggregated parameters of the models are calculated and used for simulation studies. The frequency control system presented here consists of two loops, primary frequency control on conventional generating units through governors and secondary frequency control (AGC) on selected generating units. As the paper is focused on the development of modelling, only simple controllers are employed: speed droop in the primary loop and integral controller in the AGC loop. The rest of the paper is organized as follows. Section II presents description of the Egyptian power system. Section III provides modelling of the system including model structure and derivation of weighted-average parameters. Section IV presents simulation studies and results. Section V summaries the main conclusions.

II. System Description

Fig. 1 shows the annual growth in demand in the Egyptian grid [7]. The transmission system is fed from the power stations listed in Table I, based on 2022 data. Where the simulated equivalent Egyptian grid consists of 280 generation units in 61 power plants with variation in the rating. The three large power plants (SIEMENS) at New Capital, Beni Suif and Burllus are included. Renewable power plants including Benban, Kurimat solar, Gabl Elzeet, Lakila, Shokir and Zafrana 1 & 2 as listed in Table II. The loads are simulated based on the 2022 Summer peak load which is 33 GW, and the 2022 winter minimum load which is 17.5 GW, according to the Egyptian Electricity Holding Company annual reports [7].

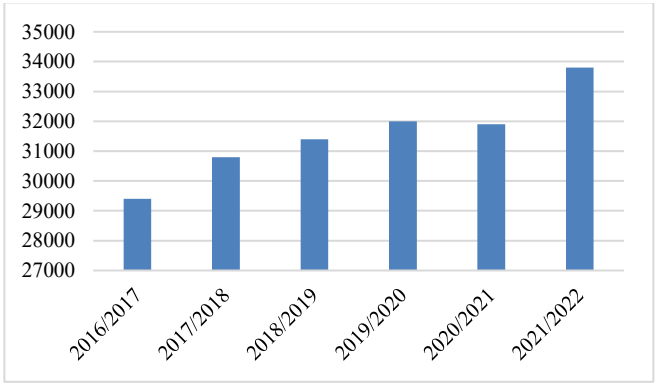

Fig. 1. Annual load development

2024 14th International Conference on Electrical Engineering (ICEENG) | 979-8-3503-4342-7/24/$31.00 ©2024 IEEE | DOI: 10.1109/ICEENG58856.2024.10566425

TABLE I. POWER STATIONS IN EGYPTIAN POWER GRID - 2022 DATA

Power Station	Capacity (MW)	Governor
High Dam	12×175 HT	HYGOV
Aswan Dam	7×40 HT + 4×67.5 HT	HYGOV
Isan	6×14.28 HT	HYGOV
Naga Hamady	4×16 HT	HYGOV
Assiut	4×8 HT	HYGOV
Walid	2×300 ST	TGOV1
Assiut Walidia	1×650 ST	TGOV1
Kurimat 1	2×627 ST	TGOV1
Kurimat2	2×250 GT + 1×250 ST	GAST+TGOV1
Kurimat 3	2×250 GT + 1×250 ST	GAST+TGOV1
West Assyut	8×125 GT + 2×250 ST	GAST+TGOV1
Beni Suif	8×400 GT + 4×400 ST	GAST+IEEEG1
Suez Boot	2×341.25 ST	TGOV1
Sokhna	2×650 ST	TGOV1
Helwan South	3×650 ST	TGOV1
Ataka	4×150 ST+2*300 ST	TGOV1
New Ataka	2×156 GT + 2*164 GT	GAST
Abo Soltan	4×150 ST	TGOV1
New Shabab	8×125 GT + 2×250 ST	GAST+TGOV1
Oun Mousa	2×320 ST	TGOV1
Suez Thermal	1×650 ST	TGOV1
Arish	2×33 ST	TGOV1
Port Said Boot	2×341 ST	TGOV1
Sharm	6×48 GT	GAST
Hurgada	6×48 GT	GAST
Cairo South	1×110 GT + 1×55 ST	GAST+TGOV1
New Capital	8×400 GT + 4×400 ST	GAST+IEEEG1
Tebbin	2×350 ST	TGOV1
Cairo West	2×330 ST+2×350 ST	TGOV1
Cairo West New	1*650 ST	TGOV1
Shobra	4×315 ST	TGOV1
Cairo North	4×250 GT + 2×250 ST	GAST+TGOV1
6 October	4×150 GT	GAST
Ext. October	4×150 GT + 1×318.7 ST	GAST+TGOV1
North Giza	6×250 GT + 3×250 ST	GAST+TGOV1
Demiatta	6×132 GT + 3×136 ST	GAST+TGOV1
New Demiatta	4×125 GT	GAST
West Demiatta	4×125 GT + 1×250 ST	GAST+TGOV1
Ext. W. Demiatta	4×125 GT + 1×250 ST	GAST+TGOV1
Tlkha 750	2×250 GT + 1×250 ST	GAST+TGOV1
Tlkha 210	2×210 ST	TGOV1
Alatf	2×250 GT + 1×250 ST	GAST+TGOV1
New Mahmdia	2× 186 GT	GAST
Matroh	2×30 ST	TGOV1
Damnhour 300	1×300 ST	TGOV1
Kafr Dawar	2×110 ST	TGOV1
Banha	2×250 GT + 1×250 ST	GAST+TGOV1
Nobaria	6×250 GT+3×250 ST	GAST+TGOV1
Abo Kir 220	4×150 ST + 1×311 ST	TGOV1
Abo Kir 500	2×650 ST	TGOV1
Burllus	8×400 GT + 4×400 ST	GAST+IEEEG1
Sidi Krir 1	2×320 ST	TGOV1
Sidi Krir 2	2×341 ST	TGOV1
Sidi Krir 500	2×250 GT + 1×250 ST	GAST+TGOV1

TABLE II. RENEWABLE STATION IN EGYPTIAN POWER GRID- 2022 DATA

Power Station	Capacity (MW)	Type
Benban	1465	PV
Kurimat Solar	140	Thermal/Solar
Gabl Elzeet	580	Wind
Lakila	249.6	Wind
Shokir	262.5	Wind
Zafarana 1 &2	541.1	Wind

A full model of the system is described in [8]. Currently, the Egyptian grid is connected to Libya power grid (at 220 kV level), to Jordon power grid (at 500/400 kV level) and to Sudan power grid (at 220 kV level). In near future it will be connected to Saudi Arabia grid through a DC link to exchange 3000 MW.

III. SYSTEM MODELING

A. Types of Generating Units

The generating units of the Egyptian grid are driven by various types of prime movers including gas turbines, steam turbines, hydro turbines, combined cycle in addition to wind turbines. The type of solar power plant at Benban solar power plant is based on Photovoltaic (PV) system. Each type of conventional generator has its own governor to keep the frequency within the permissible ranges according to Grid Code [10]. Governor models are simulated with equivalent weighted-average parameters derived from actual data. The model of the system consists of five parts. The GAST model is used to represent all gas turbine and speed-governor systems as illustrated in Fig. (2) [11]. The TGOV1 model is used to represent steam turbine prime mover systems as illustrated in Fig. (3) [11]. These include conventional separate steam turbines or that part in a combined cycle configuration. In the combined cycle power plant, the governor valve of the steam part is made insensitive to frequency variations, since the frequency response is usually achieved through the speed governor of the gas turbine part. In the combined cycle SIEMENS generating units, the steam part is represented by the IEEEG1 model illustrated in Fig. (4) [11]. Also, HYGOV model is used to represent hydro turbine prime mover systems as illustrated in Fig. (5) [11].

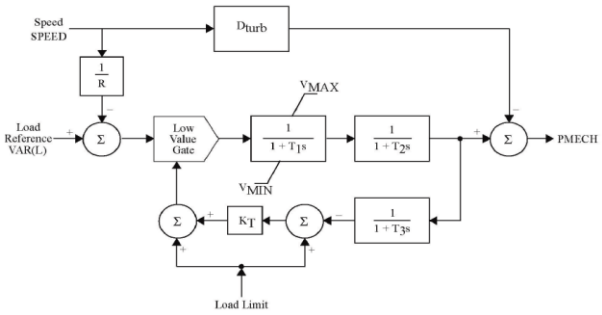

Fig. 2. GAST model [11]

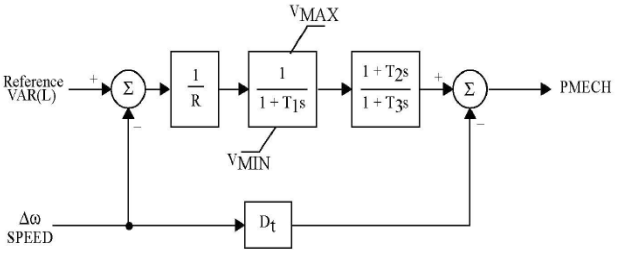

Fig. 3. TGOV1 model [11]

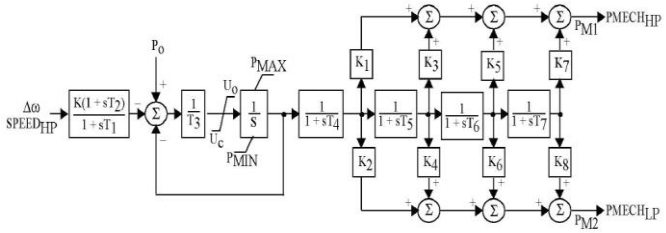

Fig. 4. IEEEG1 model [11]

B. Inertia and Damping of the System

Each generator has an inertia H_i depending on its capacity. The equivalate inertia (H) of the system depends on the online units and is calculated as follows [6], [12]:

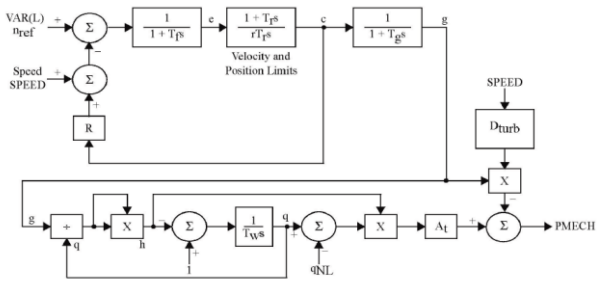

Fig. 5. Hydro Model [11]

$$H = \frac{\sum_{i=1}^{n} H_i \times MVA_i}{\sum_{i=1}^{n} MVA_i} \quad (1)$$

Where,

H_i : online units' inertia constant (sec.)
$MVAi$: MVA of online unit i
n : number of online generators

The damping constant is expressed as a percentage change in load for one percentage change in frequency. Typical values of D are 1 to 2 percent. Here, it is assumed that D = 1%.

C. Participation of Generators in Frequency Control

The contribution factor (CF) of each lumped generator is calculated as follows:

$$CF_g = \frac{\sum_{i=1}^{ng} MVA_{gas,i}}{MVA} \quad (2)$$

$$CF_s = \frac{\sum_{i=1}^{ns} MVA_{steam,i}}{MVA} \quad (3)$$

$$CF_{sg} = \frac{\sum_{i=1}^{nsg} MVA_{s-gas,i}}{MVA} \quad (4)$$

$$CF_{ss} = \frac{\sum_{i=1}^{nss} \sum MVA_{s-steam}}{MVA} \quad (5)$$

$$CF_h = \frac{\sum_{i=1}^{nh} \sum MVA_h}{MVA} \quad (6)$$

where,

MVA: Online total MVA units
$MVA_{gas,i}$: capacity of online gas unit i
$MVA_{steam,i}$: capacity of online steam unit i
$MVA_{s-gas,i}$: capacity of online SIEMENS gas unit i
$MVA_{s-steam}$: capacity of online SIEMENS steam unit i
$MVA_{h,i}$: capacity of online hydro unit i
CF_g: contribution factor of gas units
CF_s: contribution factor of steam units
CF_{sg}: contribution n factor of SIEMENS gas units
CF_{ss}: contribution factor of SIEMENS steam units
CF_h: contribution factor of hydro units
ng, *ns*, *nsg*, *nss* and *nh*: number of gas units, number of steam units, number of SIEMENS gas units, number of SIEMENS steam units and number of hydro units, respectively.

D. Dead Band and Ramp Rate

Governors are designed not to respond to small frequency deviations, which is called governor Dead Band (DB). In this paper, the dead band is taken to be $DB = \pm 30\ mHz$.

The Ramp Rate (RR) of the generating units are taken to be:

For gas units: the RR_g = 5 MW/min.
For SIEMENS gas units: the RR_{sg} = 15 MW/min.

E. Block Diagram of the AGC System

Fig. 6 shows a block diagram of the AGC system. The AGC frequency control criterion ($\Delta f = 0$) can be achieved by using an integral controller [13]. The control signal (shown in red) from the AGC controller is transmitted to the governors of the generating units under AGC.

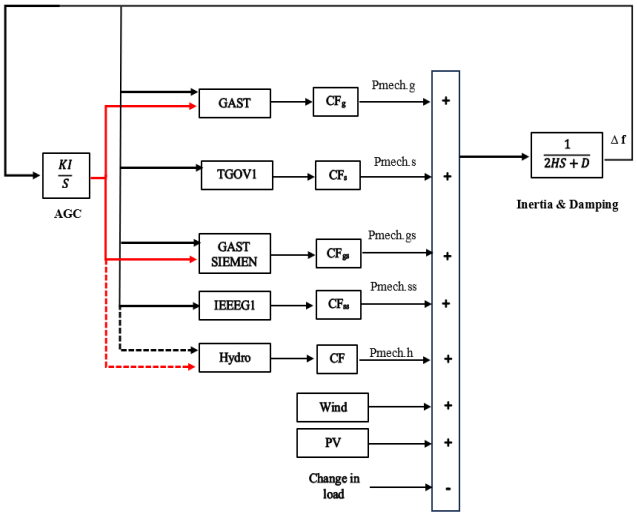

Figure (6) System block diagram

F. Parameters of Aggregated Equivalent Models

The weighted-average parameters of the aggregated equivalent models are calculated from the actual data for each type of generation and listed in Table III to Table VIII. The peak summer demand and minimum winter demand operating conditions are listed in the tables based on actual data.

TABLE III. DATA OF GAST MODEL FOR PEAK AND MINIMUM CASE

GAST	Peak	Minimum
R	0.05	0.05
T1	0.2	0.2
T2	0.1	0.1
T3	2	2
Ambient Temperature	1	1
KT	3	3
Vmax	0.76	0.76
Vmin	0	0
Dturb	0	0

TABLE IV. DATA OF GAST SIEMENS MODEL FOR PEAK AND MINIMUM CASE

GAST SIEMENS	Peak	Minimum
R	0.05	0.05
T1	0.2	0.2
T2	0.1	0.1
T3	2	2
Ambient Temperature	1	1
KT	3	3
Vmax	0.73	0.73
Vmin	0	0
Dturb	0	0

TABLE V. DATA OF TGOV1 MODEL FOR PEAK AND MINIMUM CASE

TGOV1	Peak	Minimum
R	0.05	0.05
T1	0.14	0.14
V Max	0.77	0.73
V Min	0	0
T2	2.27	2.24
T3	2	2
Dt	0	0

TABLE VI. DATA OF IEEEG1 MODEL FOR PEAK AND MINIMUM CASE

IEEEG1	Peak	Minimum
K	20	20
T1	0.2	0.2
T2	1	1
T3	0.6	0.6
Uo	0.3	0.3
Uc	-0.3	-0.3
Pmax	0.8	0.8
Pmin	0	0
T4	0.6	0.6
K1	0.3	0.3
K2	0	0
T5	0.5	0.5
K3	0.25	0.25
K4	0	0
T6	0.8	0.8
K5	0.3	0.3
K6	0	0
T7	1	1
K7	0.15	0.15
K8	0	0

TABLE VII. DATA OF HYGOV MODEL FOR PEAK AND MINIMUM CASE

HYGOV	Peak	Minimum
R	0.03	0.03
r	0.23	0.24
Tr	5	5
Tf	0.05	0.05
Tg	0.5	0.5
VELM	0.2	0.2
GMAX	0.9	0.9
GMIN	0	0
TW	1	1
At	1.17	1.17
Dturb	0.34	0.34
qNL	0.08	0.08

TABLE VIII. POWER SYSTEM DATA OF PAEK AND MINUMUM CASE

DATA	Peak	Minimum
H (Sec.)	4.08	4.36
D (p.u)	0.6381	0.4585
KI	2	2
Change in load (p.u)	0.0307	0.0307
CFg	0.27	0.25
CFs	0.47	0.39
CFsg	0.17	0.24
CFss	0.09	0.12
CFh	0	0
DB (p.u)	±0.006	±0.006
RR g (p.u)	0.02	0.02
RR gs (p.u)	0.0375	0.0375

Differences in the values highlighted in yellow in the tables are due to the number and loading of online units (i.e., the actual generating units in service) in each operating case. Table IX shows the active power of each generation type and the reserve in peak and minimum demand cases, noting that the reserve represents the spinning and standby.

TABLE IX. ACTIVEPPOWER AND RESRVE OF DIFFERENT GENERATION TYPES

Generation Type	Peak Demand		Minimum Demand	
	Power (MW)	Reserve (MW)	Power (MW)	Reserve (MW)
GAS	8936	1104	4750	1795
GAS Siemens	5900	500	3840	2560
Steam	13576.6	1529.5	580	674
Steam Siemens	2800	400	1920	1280
Hydro	992.3	1525.5	5910	2720

IV. SIMULATION STUDIES AND RESULTS

To study the sensitivity of the developed model to changes in the operating conditions, two extreme operation points in the real Egyptian Grid, are considered:

- Peak summer case with actual load 33 GW.
- Minimum winter case with actual load 17.5 GW.

In the first case (at peak demand), we assume a sudden load increase of 1000 MW (0.0307 p. u). Similarly, in the second case at minimum demand, a disturbance of sudden load increase of ≃522 MW (0.0307 p. u) is assumed. In both cases the dead band and units ramp rates given before are taken into consideration. Fig. 7 shows the frequency responses to the sudden load increase of 0.0307 p. u at peak and minimum demands. Only primary frequency control is applied to the thermal units (gas and steam) with governor speed droop characteristics. The two responses are close to each other with small differences in the nadir and steady-state frequencies. With the primary frequency control only, the system is stabilized but not return to the normal operating conditions (50±0.05% Hz) according to the grid code [10]. Table X shows a comparison between the frequency responses of Fig. 7 at peak and minimum operating conditions. The difference in nadir frequency is 0.0087 Hz and the difference in the steady-state frequency is 0.0081 Hz.

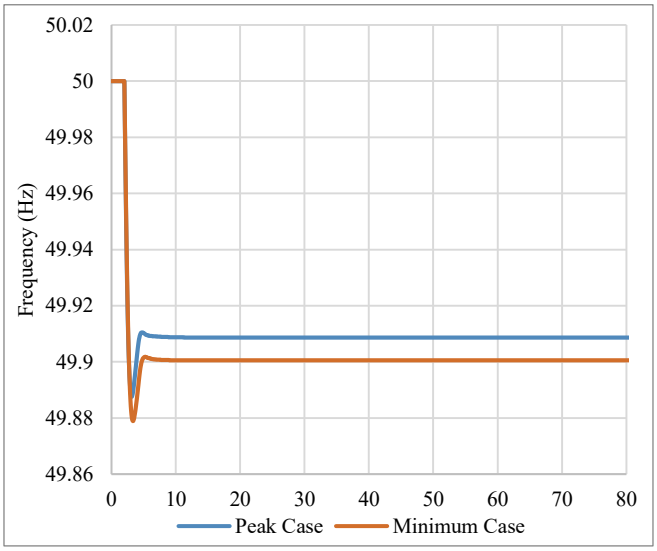

Fig. 7. Comparison frequency response with primary frequency control.

TABLE X. COMPARISON BETWEEN PEAK & MINIMUM CASES WITH PRIMARY FREQUENCY CONTROL ONLY

Case	Nadir Frequency (HZ)	Steady-State Frequency (HZ)
Peak	49.8876	49.9087
Miumum	49.8789	49.9006

Fig. 8 shows the active power contribution of each type of generating units at peak demand case. The 1000 MW added load is supplied from the generators under the primary frequency control. In the operating scenario depicted in Fig. 7 and Fig. 8, the thermal units are employed for frequency control, while the renewable energy sources (hydro, wind and PV) are not. This is to facilitate maximizing the contribution of the renewable generation [14], [15], each within its constraints. Hydro units are normally operated depending on irrigation constraints as discharge, levels and water content.

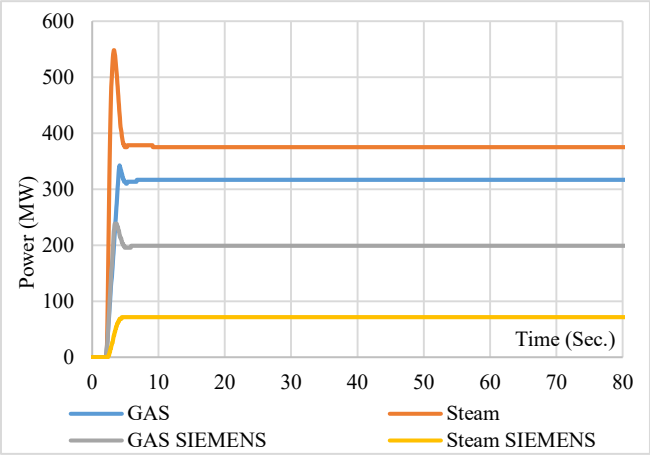

Fig. 8. Response of different governor model at peak scenario with primary frequency.

In emergency conditions, the hydro units can be manually controlled. The wind generation units operate at its maximum operating point depending on the availability of wind. During the day, the PV generation is operated at its maximum power, depending on the available solar radiation. Noting that, the two operating conditions considered here, the output of the PV generation is zero. This is because the peak demand in Egypt occurs after sunset and the minimum demand occurs before sunrise.

The rest of the results are concentrated on the AGC with the scenarios 2 and 3 summarized in Table XI. Scenario 1 is the previous case with primary frequency control only.

TABLE XI. STUDY SCENARIOS WITH AGC

Scenario	Primary Frequency Control					AGC				
	Gas	Gas Siemens	Steam	Steam Siemens	Hydro	Gas	Gas Siemens	Steam	Steam Siemens	Hydro
1	√	√	√	√						
2	√	√	√	√		√	√			
3	√	√	√	√	√	√	√			√

Fig. 9 shows the frequency responses to 0.0307 p. u sudden increase in load in Scenario 2 with the AGC the gas units as depicted in Table XI, all thermal units have primary frequency control. Both peak and minimum demand cases are shown. Again, the frequency responses are very close, confirming the validity of the proposed model in a wide range of operating conditions. Table XII shows a comparison of the two cases.

TABLE XII. COMPARISON BETWEEN PEAK & MINIMUM CASES WITH AGC

Case	Nadir Frequency (HZ)	Steady-State Frequency (HZ)
Peak	49.8876	50
Miumum	49.8789	50

With the AGC integral controller, the frequency returns to its nominal value of 50 Hz. The gain of the AGC integral controller is selected to provide slower response than the primary frequency control according to the regulations of practical power system operation [16]. In this study the value of K_I is selected to be 2.

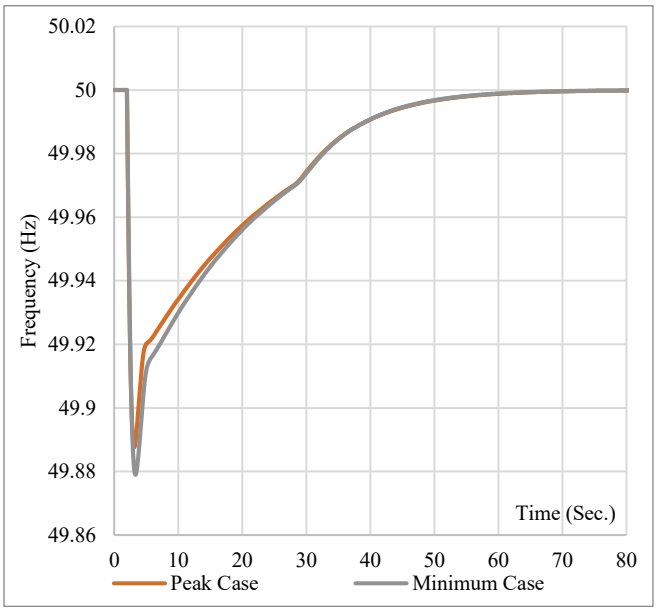

Fig. 9. Comparison frequency response with FC & AGC – Scenario 2.

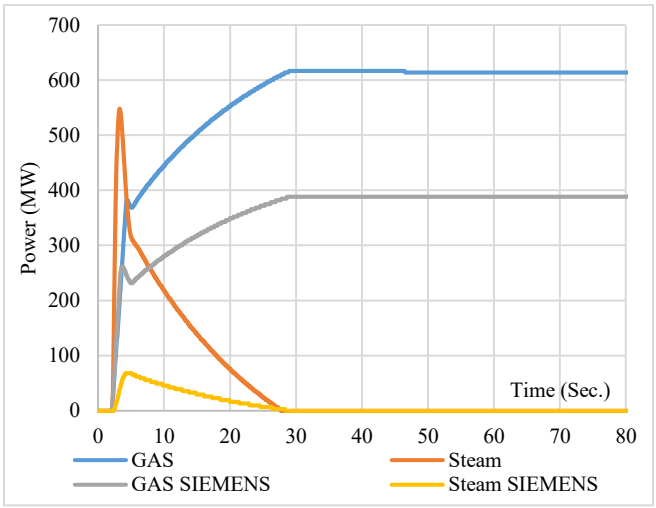

Fig. 10. Response of different governor model at peak scenario with FC &AGC – Scenario 2.

Fig. 10 shows the active power contribution of each type of generating units at peak demand case. Initially, all units under primary frequency control participate in the frequency correction. Eventually, the 1000 MW added load is supplied from the generators under the AGC, namely the gas generating units.

Fig. 11 shows the frequency response in Scnario 3, and Fig. 12 shows the contribution of each generation type in overcomming the 1000 MW increase in the load. In this scenario, the AGC is applied on the gas, gas Siemens and hydro generating units. All units have primary ferquency control as indicated in Table XI. Now, the 1000 MW added load is covered by the gas, gas Siemens and hydro units as shown in Fig. 12. The contribution of the the hydro units is the lowst compared to the contributions of the gas units.

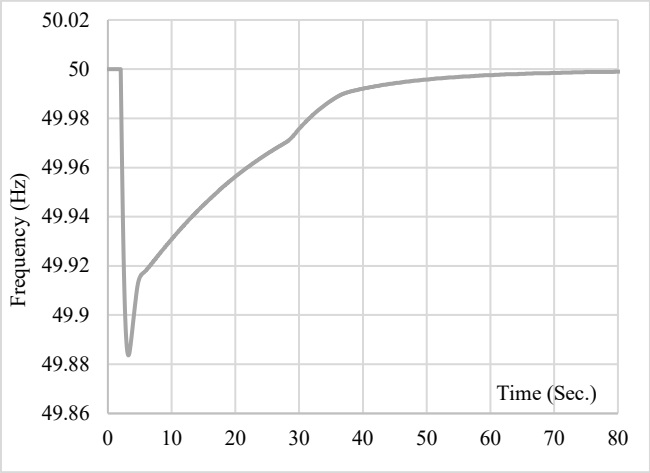

Fig. 11. Frequency response for gas & hydro units under AGC - Scenario 3.

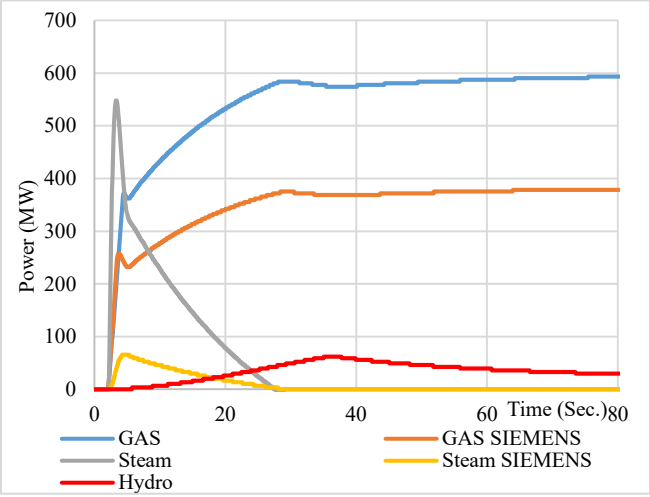

Fig. 12. Response of different governor model at peak scenario with FC &AGC on gas & hydro Scenario 3

V. Conclusions

A dynamic model of the Egyptan grid is developed for AGC studies based on real data. The model represets all types of generating units, each category is combined in a lumped large genrating unit with approperiate model of turbine and speed governor system. The simulation results proves the validity of the model for AGC studies over a wide range of operating conditions. Three AGC scenarios are considered: namely, (i) primary ferequency control on all units, (ii) AGC on gas units, and (iii) AGC on gas and hydro units.

With currently low share of renewable energy resources, the studies in this paper have considered the application of the AGC to conventional generating units only, in particular gas units, and operate the renewable sources (hydro, wind and PV) at their maximum available power with no contribution in frequency control. In future, with planned high share of renewable energy sources, it is recommended to investigate the possibility of considering their contribution in the AGC.

References

[1] N. Jaleeli, et al., “Understanding Automatic Generation Contro”, Report of the AGC Task Force of the IEEE/PES/PSE/System Control Subcommittee, IEEE Transactions on Power Systems, vol. 7, no. 3, pp. 1106-1122, August 1992.

[2] A. Keyhani , and A. Chatterjee, “Automatic generation control structure for smart power grids”, IEEE Transactions on Smart Grid, **3** (3): pp. 1310-1316, 2012.

[3] M .M. Hussein, et al., “Advanced Frequency Control Technique Using GTO with Balloon Effect for Microgrids with Photovoltaic Source to Lower Harmful Emissions and Protect Environment”, Sustainability 2024, 16, 831. https://doi.org/10.3390/su16020831

[4] ENTSO-E, “Policy 1: Load-Frequency Control and Performance [C]” European Network of Transmission System Operators for Electricity. https://eepublicdownloads.entsoe.eu/clean-documents/pre2015/publications/entsoe/Operation_Handbook/Policy_1_Appendix%20_final.pdf

[5] O. I. Elgerd, “Electric Energy Systems Theory: An Introduction”, McGraw-Hill, New York, 1971.

[6] P. S. Kundur, “Power system stability and control” 2nd Edition, McGraw-Hill, New York, 2022.

[7] Egyptian Electricity Holding Company, “Annual Report 2021/2022” http://www.moee.gov.eg/english_new/EEHC_Rep/REP2021-2022en.pdf

[8] O. H. Abdalla, A. M. Abdel Ghany, and H. H. Fayek, “Development of a Digital Model of the Egyptian Power Grid for Steady-State and Transient Studies”, Proc. of the 11th International Conference on Electrical Engineering, Paper No. 83-EPS, Military Technical College, Cairo, Egypt, 3-5 April, 2018.

[9] O. H. Abdalla, H. H. Fayek, and A. M. Abdel Ghany, "Steady-State and Transient Performances of the Egyptian Grid with Benban Photovoltaic Park", Proc. Cigre Egypt 2019 Conference, The Future of Electricity Grids - Challenges and Opportunities, Paper No. 205, 6-8 March 2019, Cairo, Egypt. http://works.bepress.com/omar/66/

[10] Transmission Grid Code, Egyptian Electricity Transmission Company, EETC, Cairo, Egypt. http://www.eetc.net.eg/grid_code.html

[11] P. Pourbeik, et al., “Dynamic models for turbine-governors in power system studies”, Task Force on Turbine-Governor Modeling, Technical Report EPS-TR1, IEEE Power Energy Society, January 2013.

[12] Q. Shia, F. Lia, Q. Hub, Z. Wang, “Dynamic demand control for system frequency regulation: Conceptreview, algorithm comparison, and future vision”, Electric Power Research, Elsevier, Vol. 154, pp. 75-87, 2018. http://dx.doi.org/10.1016/j.epsr.2017.07.021

[13] H. A. Yousef, “Power system load frequency control: classical and adaptive fuzzy approaches” 2017: CRC Press

[14] H. H. Fayek, and O. H. Abdalla, “Maximization of Renewable Power Generation for Optimal Operation of the Egyptian Grid”, the 29th IEEE International Symposium on Industrial Electronics ISIE’20, 17-19 June 2020. https://ieeexplore.ieee.org/document/9152450

[15] H. H. Fayek, and O. H. Abdalla, "Operation of the Egyptian Power Grid with Maximum Penetration Level of Renewable Energies Using Corona Virus Optimization Algorithm" Smart Cities, Vol. 5, No. 1, pp. 34-53, 5 January, 2022, https://www.mdpi.com/2624-6511/5/1/3

[16] EPRI, “EPRI Power Systems Dynamics Tutorial: 2020 Edition” Electric Power Research Institute, Product ID: 3002018947, Nov. 2020. https://www.epri.com/research/products/000000003002018947